

The decreasing albedo of Zhadang glacier on western Nyainqntanglha and the role of light-absorbing impurities

B. Qu^{4,1}, J. Ming^{1,2,3}, S.-C. Kang^{1,4}, G.-S. Zhang⁴, Y.-W. Li⁴, C.-D. Li⁴, S.-Y. Zhao⁵, Z.-M. Ji⁴, and J.-J Cao⁵

1 State Key Laboratory of Cryospheric Sciences, Cold and Arid Regions Environmental and Engineering Research Institute, Chinese Academy of Sciences, Lanzhou, China

2 Collaborative Innovation Center on Forecast and Evaluation of Meteorological Disasters, Nanjing University of Information Science & Technology, Nanjing, China

3 National Climate Center, China Meteorological Administration (CMA), Beijing, China

4 Key Laboratory of Tibetan Environment Changes and Land surface Processes, Institute of Tibetan Plateau Research, Chinese Academy of Sciences, Beijing, China

5 State Key Laboratory of Loess and Quaternary Geology, Institute of Earth Environment, Chinese Academy of Sciences, Xi'an, China

Corresponding author: J. Ming (petermingjing@hotmail.com)

Abstract

The large change in albedo has a great effect on glacier ablation. Atmospheric aerosols (e.g. black carbon (BC) and dust) can reduce the albedo of glaciers and thus contribute to their melting. In this study, we investigated the measured albedo as well as the relationship between albedo and mass balance in Zhadang glacier on Mt. Nyanqntanglha associated with MODIS (10A1) data. The impacts of BC and dust in albedo reduction in different melting conditions were identified with SNOW ICe Aerosol Radiative (SNICAR) model and in-situ data. It was founded that the mass balance of the glacier has a significant correlation with its surface albedo derived from Moderate Resolution Imaging Spectroradiometer (MODIS) onboard Terra satellite. The average albedo of Zhadang glacier from MODIS increased with the altitude and fluctuated but overall had a decreasing trend during 2001–2012, with the highest (0.722) in 2003 and the lowest (0.597) in 2009 and 2010, respectively. **Snow samples were collected to measure BC and dust in Zhadang glacier in the summer of 2012.** The sensitivity analysis via SNICAR showed that BC was a major factor in albedo reduction when the glacier was covered by newly fallen snow. Nevertheless, the contribution of dust to albedo reduction can be as high as 58% when the glacier experienced strong surficial melting that the surface was almost bare ice. And the average radiative forcing (RF) caused by dust could increase from 1.1 to 8.6 W m^{-2} exceeding the forcings caused by BC after snow was deposited and surface melting occurred in Zhadang glacier. This suggest that it may be dust rather than BC, dominating the melting of some glaciers in the TP during melting seasons.

1. Introduction

1 Glaciers and snow cover are important reservoirs of fresh water on Earth. A rough volume of
2 $2.4 \times 10^7 \text{ km}^3$ of water is stored in them (Oki and Kanae, 2006) and changes in these reservoirs
3 have a great effect on water supply in many regions of the world (Mote et al., 2003; Yao et al.,
4 2012). The Tibetan Plateau (TP) is the source of many great rivers (e.g. Yangtze, Yellow,
5 Indus, Ganges, and Brahmaputra rivers), whichconcentrate their sources at the glaciers in the
6 TP known as the “Asian Water Towers”. More than 1.4 billion people depend on the water
7 from these rivers (Immerzeel et al., 2010), but these glaciers here have been undergoing rapid
8 changes (Kang et al., 2010; Yao et al., 2012). Therefore, it is important to understand the
9 impact factors that affect the glaciers and snow cover.

10

11 The surface energy budget of glaciers has significant effects on their ablation (Zhang et al.,
12 2013), and snow/ice albedo is one of the most important parameters that affect the absorbed
13 radiation. Snow/ice albedo is defined as the fraction of the reflected and the incident radiant
14 flux in the surface of the snow/ice. A higher albedo implies cleaner snow surface or less
15 energy available for melting. Clean snow has the highest albedo (as high as 0.9) of any natural
16 substance but this diminishes when snow surfaces are dirty or darkened **due to snow grain**
17 **size increases** (Warren and Wiscombe, 1980; Wiscombe and Warren, 1980). A recent report
18 (Lhermitte et al., 2012) indicates a darkening surface of the Greenland ice sheet and a rapidly
19 decreasing albedo during 2000–2011, which will greatly increase the rate of mass loss of the
20 ice sheet as more solar energy is absorbed by the darker glacial ice (Farmer and Cook, 2013).

21

22 It is widely recognized that temperature, precipitation and glacial dynamic processes are the
23 key factors that affect glacial change (Sugden and John, 1976). However, there is now a
24 general consensus that light-absorbing constituents (LACs, e.g. BC and dust) can reduce the
25 albedo of glaciers (dirtying or darkening effect) and thus also contribute to the mass loss of
26 glaciers. Both BC and dust are important absorbers of solar radiation in its visible spectra
27 (Warren and Wiscombe, 1980; Hadley and Kirchstetter, 2012; IPCC, 2007), and BC has an
28 absorbing capacity ~ 50 to 200 times higher than dust (Warren and Wiscombe, 1980). The
29 impacts of BC and dust deposited on the TP glaciers (in particular, on their radiation balance)
30 have been reported in the previous literatures (Ming et al., 2009a, 2013a). The simulation on

1 the effect of LACs on the albedo of the Himalayan glaciers showed that LACs in this region
2 had a contribution of 34% to the albedo reduction during the **late** spring time, with 21% from
3 BC, and 13% originating from dust (Ming et al., 2012).

4

5 The lowering of surface albedo due to the presence of a dust layer could also lead to a drastic
6 increase in the glacier melting rate during the melting season (Fujita, 2007). In general, BC
7 can be transported over long distances (Ming et al., 2010), while dust usually comes from the
8 local or regional environment of the glaciers (Kang et al., 2000). Historical deposition records
9 of BC revealed by ice cores and lake sediments over the TP, indicate that BC originating from
10 south and central Asia have inevitably reached the glaciers in recent decades (Ming et al.,
11 2008; Xu et al., 2009b; Cong et al., 2013).

12

13 There have been extensive researches focusing on quantifying the impacts of LACs in ice
14 cores and snow cover to understand the relationship between LACs and albedo reduction
15 (Aoki et al., 2011; Painter et al., 2007, 2012; Ginot et al., 2013; Kaspari et al., 2013).
16 However, few researchers discussed the exact effects that BC and dust take on different types
17 of glacier surfaces during the melting season; Dust sometimes causes dramatic spatial
18 variation of surface albedo in glaciers. Moreover, glacier melting causes LAC particles to
19 concentrate in the surface and to further enhance absorbing the radiation. This positive
20 feedback highlights the importance of investigating LACs and their effects on albedo and
21 glacial melt across a whole glacier, particularly in a prevailing situation where glaciers are
22 shrinking and emissions of BC are increasing (Bond et al., 2013). In this work, we investigate
23 the spatial distribution of LACs from the terminite along to the accumulation zone of
24 Zhadang glacier, southern TP during the summer of 2012 and estimate the contribution of BC
25 and dust to the albedo reduction in different melting conditions.

26

27 **2. Methodology**

28 The Zhadang glacier is located in western Nyainqntanglha, southern TP, (30°28.57'N,
29 90°38.71'E, and 5500-5800 m a.s.l.) (Fig. 1). Surface snow/ice samples were collected and
30 surface albedo was observed on Zhadang glacier during 12-16 July and 24-27 August, 2012.
31 We classified three conditions or scenarios of the glacier surface: (1) S-I: the surface of the

1 glacier is bare ice containing some visible dark constituents (Fig. 2a); (2) S-II: the surface is
2 covered by aged snow/firn (Fig. 2a); (3) S-III: the surface is covered by fresh snow (Fig. 2b).
3 These surface conditions are typical in most alpine glaciers all around the year (Benn and
4 Evans, 2010). The description of sampling details in Zhadang glacier is given in Table 1.
5

6 **2.1 Albedo data from the Moderate Resolution Imaging Spectroradiometer**
7 **(MODIS) onboard Terra**

8 The MODIS albedo data were used to investigate the albedo change in Zhadang glacier. The
9 series of the product is MODIS/Terra Snow Cover Daily L3 Global 500m Grid (MOD10A1),
10 which are based on a snow mapping algorithm that employs a normalized difference snow
11 index (NDSI) and other criteria tests (Riggs and Hall, 2011). MOD10A1 product contains
12 four data layers: snow cover, snow albedo, fractional snow cover, and **binary** quality
13 assessment (QA) **assigned as “good” or “bad”**. They are compressed in hierarchical data
14 format-Earth observing system (HDF-EOS) formatted along with corresponding metadata.
15 The images of MOD10A1 are 1200 km by 1200 km tiles with a resolution of 500 m × 500 m
16 gridded in a sinusoidal map projection. Data are available from 24 February 2000 to present
17 via FTP (Hall et al., 2006). The snow albedo data that used to calculate are based on three
18 criteria **applied**: the pixels are identified as snow cover, fractional snow cover is 100, and the
19 pixels pass the QA. MODIS daily albedo has high accuracy in flat terrain (Stroeve et al., 2006;
20 Tekeli et al., 2006.), while it shows some errors in complex topography such as mountainous
21 regions (Sorman et al., 2007; Warren, 2013).

22
23 In order to verify the applicability of MOD10A1 product in Zhadang glacier, we use the
24 observed data measured by the Kipp & Zonen radiometers mounted on an automatic weather
25 station (AWS), which was set in the saddle of the glacier (5680 m a.s.l., Fig. 1). The albedo
26 data was extracted from the precise pixel in the relevant MODIS image where the AWS
27 located. The observed albedo were selected in the local time period of 12:30 to 13:30 LT,
28 considering the right scanning time of Terra satellite passing over the study area. The
29 correlation analysis between the MODIS data and observed data showed a good relationship
30 at the confidence level of 0.02 (Fig. 3), indicating that it is reasonable to use MOD10A1 data
31 to study to albedo change of Zhadang glacier.

1 **2.2 Field albedo observation**

2 Warren (2013) suggested that it is unlikely to detect the impact of black carbon on snow
3 albedo by remote sensing. In this work, a spectroradiometer (Model ASD® FS-3) was used to
4 measure the spectral albedo of the glacier. This covers a radiation waveband of 350-2500 nm
5 with a wavelength resolution of one nanometre. The optical sensor of the spectroradiometer
6 was set up in a pistol-shape device that the optical fibre can be fixed inside and mounted on
7 the rocker arm of the tripod with a gradienter for levelling. The distance of the sensor and the
8 snow surface was approximately 0.5 m allowing to measure the spectral reflectances. During
9 the expedition of July 2012, we measured surface albedo and collected snow samples in S-I
10 (two sites: A and B) and S-II (C and D) conditions. In August, the glacier was covered by
11 newly fallen snow, and albedo and surface snow samples were successfully observed and
12 collected at eight sites in S-III condition (Fig. 2). Along with the sampling, other necessary
13 parameters such as snow density, grain sizes, and etc. for simulating the surface albedo were
14 also observed. Details concerning the simulations of surface albedo have been introduced in a
15 previous work (Ming et al., 2013a).

16 **2.3 Snow/ice sampling and BC/dust measurement**

17 Snow/ice samples were collected in accordance with the “Clean hands-Dirty Hands” principle
18 meaning the one whose hands are collecting sampling won’t touch any other material that
19 may contaminate snow samples (Fitzgerald, 1999). We collected two parallel samples 10 cm
20 away from each other from surface to 5-cm depth at each site when measuring albedo. Snow
21 density was measured using a balance. The samples were stored in NALGENE® HDPE
22 wide-mouth bottles (250 mL) and kept in frozen condition until laboratory analysis. The snow
23 grain sizes were measured using a hand lens (25X) with accuracy of 0.02 mm; the largest
24 length of a single ice crystal was also measured using a snow crystal card with 1 mm grids
25 (Aoki et al., 2007). We filtered the snow melt water through quartz-fiber filters, which were
26 weighed before and after the filtration using a microbalance to evaluate the mass of on-load
27 dust. A thermal-optical method of carbon analysis, using DRI® Model 2001A OC/EC (Chow
28 et al., 1993) was employed to measure BC mass in the samples.

29 **2.4 Albedo reduction modelling and radiative forcing (RF)**

30 The Snow-Ice-Aerosol-Radiative (SNICAR) model can be used to simulate the hemisphere
31 albedo of snow and ice for unique combinations of impurity contents (BC, dust, and volcanic

1 ash), snow grain size, and incident solar flux characteristics (Flanner et al., 2007). It was
2 applied to simulate the albedo varying caused by BC and dust deposited in the glacier surface
3 in this work. We conducted a series of sensitivity analysis to identify the impact of BC and
4 dust on albedo reduction in three different surface conditions of Zhadang glacier (also see
5 Section 2.2). Solar zenith angle was identified based on the time and position of specific
6 sampling sites. Snow grain effective radius is taken as the half of observed snow grain size
7 introduced by Aoki et al., (2007) and shown in Table 1. The albedo of the underlying bare ice
8 is taken as 0.11-0.19 in the visible band and 0.18-0.23 in the near-infrared band as in-situ
9 measured by the spectroradiometer. We use the default value 1 as the mass absorption cross
10 section (MAC) scaling factor (experimental) in the modelling. . The detailed parameters used
11 in SNICAR are listed in the appendix.

12 RF was defined using the equation below,

13 $RF = R_{in-short} * \Delta\alpha,$

14 where $R_{in-short}$ denotes incident solar radiation measured by radiometer. , and $\Delta\alpha$ denotes the
15 reduction of albedo.

16 **3. Results and Discussions**

17 **3.1 Surface albedo variations of Zhadang glacier into the 21st century**

18 The albedo of Zhadang glacier increased with elevation (Table 1) due to the lower
19 temperature favouring more cold snow stored in higher elevations. The MODIS albedo of
20 Zhadang glacier shows an obvious decreasing trend of 0.003 a⁻¹ during 2001– 2012, in spite
21 of the inter-annual fluctuations (Fig. 4). The annually average albedo declined from 0.676 in
22 2001 to 0.597 in 2010 with a maximum of 0.722 in 2003, and a minimum of 0.597 in 2009
23 and 2010. This trend was also revealed in the Himalayan and Tanggula glaciers (Ming et al.,
24 2012; Wang et al., 2012).

25 Surface albedo of a specific glacier could be linked with its mass balance in the TP, which has
26 been proved by Wang et al. (2013). We used the observed mass balance data from 2006
27 through 2010 in Zhadang glacier (Zhang et al., 2013) and did a correlation analysis with the
28 glacier surface albedo (Fig. 4). Lower albedo is related to larger negative balances, and vice
29 versa. For example, the most negative mass balance of Zhadang glacier was appearing in
30 2010 when the albedo of the glacier reaches to the minimum, whereas the positive mass
31 balance occurred in 2008 and the albedo was the highest during 2006–2010. The significant

1 positive correlation ($n = 7$, $\alpha = 0.01$, $R^2 > 0.83$) between albedo and the mass balance of the
2 glacier indicates that the surface albedo of Zhadang glacier can be a strong index of glacier
3 mass balance.

4

5 **3.2 Impacts of BC and dust on albedo**

6 BC and dust concentrations, as well as other observations such as snow grain size, snowpack
7 density, snowpack thickness, and etc., on Zhadang glacier are shown in Table 1. In S-I
8 condition, the concentration of dust varied from 504–1892 ppm with an average of 1198 ppm,
9 while BC was 334–473 ppb with an average of 404 ppb. In S-II condition, the concentrations
10 of BC and dust ranged from 81 to 143 ppb with an average of 112 ppb, and 34 to 67 ppm with
11 an average of 50 ppm, respectively. However, the concentration of BC in S-III was 41 to 59
12 ppb with an average of 52 ppb, while the dust concentration was 3 to 8 ppm with an average
13 of 6 ppm.

14

15 There are large differences in BC and dust concentrations in the surface of Zhadang glacier in
16 different scenarios of surface features (Fig. 2a). In S-I and S-II, intensive surface melting
17 could lead to a strong enrichment of LACs in the surface of the glacier. In S-III conditions,
18 Zhadang glacier was covered by fresh snow due to frequent snowfalls at nights (Fig. 2b).
19 Thus, the concentrations of LACs in S-III are several magnitudes lower than those in S-I and
20 S-II conditions (Table 1). Table 2 provides observed and simulated albedos at the sampling
21 sites. The observed surface albedo increases roughly along with elevations on Zhadang
22 glacier, in contrast with the concentrations of BC and dust in S-I and S-II conditions. **The**
23 **correlations of in-situ observed albedo and simulated albedo by SNICAR after adding**
24 **measured BC and dust into snow surface are 0.9992 for S-I, 0.9995 for S-II, and 0.4729 for**
25 **S-III, respectively.** This suggests that the enrichment of BC and dust on the surface of the
26 glacier could reduce the glacier albedo, thus resulting in melting of glaciers.

27 The sensitivity analysis of the respective impacts of BC and dust on reducing snow albedo of
28 Zhadang glacier was calculated by SNICAR and showed in Fig. 5. **We assume that the model**
29 **also works well for thin snow (< 5 cm) with ice beneath. This configuration with the SNICAR**
30 **model implies that impurities contained within the ice beneath the snow do not contribute to**
31 **the radiative forcing calculations. It is unclear how important this assumption is, but it may**
32 **contribute to a low bias in the RF estimates.** We presume three impacting factors dominating

1 the albedo varying in the glacial surface, i.e., BC, dust, and the grain size growing due to
2 warming (Ming et al., 2012). Dust exceeding BC was the most dominant factor of reducing
3 glacier albedo in S-I. BC other than dust dominates reducing albedo in case the glacier was
4 covered by snow (S-II and S-III). The incoming solar irradiances at every sampling time
5 during the two trips are listed in Table 2.

6

7 We calculated the RF of both BC and dust on the Zhadang glacier. The simulation shows that
8 the RF caused by BC and dust deposition on Zhadang glacier varied between $0.4\text{--}11.8\text{ W m}^{-2}$
9 and $0.5\text{--}16.4\text{ W m}^{-2}$, respectively (Fig. 5). The RF of dust is much higher than that of BC in
10 S-I, while the RF of BC exceeds dust in S-II and S-III. On average, the forcing caused by dust
11 deposition on the Zhadang glacier in the summer of 2012 was $2.7\pm3.4\text{ W m}^{-2}$, and that caused
12 by BC was $4.8\pm3.2\text{ W m}^{-2}$, which is a little lower than that recorded in the northern TP (Ming
13 et al., 2013b), and higher than those recorded in the Arctic (Flanner, 2013; Dou et al., 2012).

14

15 **4. Summary and Conclusions**

16 The albedo of Zhadang glacier had been declining during the 10 years of 2001–2010
17 suggested by MODIS data and has a significant correlation with the mass balance. That
18 means remotely sensed albedo data could be used in the research of mass balance change of
19 glacier in large spatial scale. During the summer of 2012, the average concentrations of BC
20 and dust are 404 and 1198 ppm in the surface of Zhadang glacier, which were one and three
21 magnitudes higher than 52 ppb of BC and 6.4 ppm of dust in fresh snow. The effects of BC
22 and dust on the glacier albedo were quantified based both on observed and simulated data.
23 The contribution of dust and BC to albedo reduction was 58 and 27 %, respectively, when the
24 glacier was covered by bare ice. In the surface covered by aged snow, 36% of the surface
25 albedo reduction was caused by BC, and 29% was caused by dust, respectively. When the
26 glacier was covered by fresh snow, BC and dust contributed 12 and 3% to albedo decreasing,
27 respectively. BC was a major factor inducing albedo decreasing when the glacier was covered
28 by snow including the fresh and aged. Dust made the most significant contribution to albedo
29 reduction when the glacier was bare-ice covered.

30

1 Acknowledgements

2 This work was supported by the Global Change Research Program of China (2010CB951401),
3 the National Natural Science Foundation of China (Grants 41121001, 41225002, and
4 41190081), State Key Laboratory of Cryospheric Sciences, CAS (no. SKLCS-ZZ-
5 2012-01-06), CMA (no. GYHY201106023), the National Science & Technology Pillar
6 Program during the Twelfth Five-year Plan Period (2012BAC20B05), and the Climate
7 Change Science Foundation of CMA (2013-2014). The authors would like to give thanks to H.
8 Zhang for his great help on processing the albedo data.

References

Aoki, T., Hori, M., Motoyoshi, H., Tanikawa, T., Hachikubo, A., Sugiura, K., Yasunari, T. J., Storvold, R., Eide, H. A., and Stamnes, K.: ADEOS-II/GLI snow/ice products—Part II: Validation results using GLI and MODIS data, *Remote Sensing of Environment*, 111, 274-290, 10.1016/j.rse.2007.02.035, 2007.

Aoki, T., Kuchiki, K., Niwano, M., Kodama, Y., Hosaka, M., and Tanaka, T.: Physically based snow albedo model for calculating broadband albedos and the solar heating profile in snowpack for general circulation models, *Journal of Geophysical Research: Atmospheres* (1984–2012), 116, 2011.

Benn, D. I., and Evans, D. J.: *Glaciers and glaciation*, Hodder Education, 2010.

Bond, T., Doherty, S., Fahey, D., Forster, P., Berntsen, T., DeAngelo, B., Flanner, M., Ghan, S., Kärcher, B., and Koch, D.: Bounding the role of black carbon in the climate system: A scientific assessment, *Journal of Geophysical Research: Atmospheres*, 10.1002/jgrd.50171, 2013.

Chow, J. C., Watson, J. G., Pritchett, L. C., Pierson, W. R., Frazier, C. A., and Purcell, R. G.: The DRI thermal/optical reflectance carbon analysis system: description, evaluation and applications in US air quality studies, *Atmospheric Environment. Part A. General Topics*, 27, 1185-1201, 1993.

Cong, Z., Kang, S., Gao, S., Zhang, Y., Li, Q., and Kawamura, K.: Historical trends of atmospheric black carbon on Tibetan Plateau as reconstructed from a 150-year lake sediment record, *Environmental science & technology*, 2013.

Dou, T., Xiao, C., Shindell, D., Liu, J., Eleftheriadis, K., Ming, J., and Qin, D.: The distribution of snow black carbon observed in the Arctic and compared to the GISS-PUCCINI

model, *Atmospheric Chemistry and Physics*, 12, 7995-8007, 2012.

Farmer, G. T., and Cook, J.: Earth's Albedo, Radiative Forcing and Climate Change, in: *Climate Change Science: A Modern Synthesis*, Springer, 217-229, 2013.

Fitzgerald, W. F.: Clean hands, dirty hands: Clair Patterson and the aquatic biogeochemistry of mercury, *Clean Hands, Clair Patterson's Crusade Against Environmental Lead Contamination*, 119-137, 1999.

Flanner, M. G., Zender, C. S., Randerson, J. T., and Rasch, P. J.: Present-day climate forcing and response from black carbon in snow, *J. Geophys. Res.*, 112, D11202, 10.1029/2006JD008003, 2007.

Flanner, M. G.: Arctic climate sensitivity to local black carbon, *Journal of Geophysical Research: Atmospheres*, 10.1002/jgrd.50176, 2013.

Fujita, K.: Effect of dust event timing on glacier runoff: sensitivity analysis for a Tibetan glacier, *Hydrological Processes*, 21, 2892-2896, 2007.

Ginot, P., Dumont, M., Lim, S., Patris, N., Taupin, J., Wagnon, P., Gilbert, A., Arnaud, Y., Marinoni, A., and Bonasoni, P.: A 10 yr record of black carbon and dust from Mera Peak ice core (Nepal): variability and potential impact on Himalayan glacier melting, *Cryosphere Discussions*, 7, 2013.

Hall, Dorothy K., George A. Riggs, and Vincent V. Salomonson. MODIS/Terra Snow Cover Daily L3 Global 500m Grid V005, [January 2001 to December 2010]. Boulder, Colorado USA: National Snow and Ice Data Center. Digital media (updated daily), 2006

Immerzeel, W. W., van Beek, L. P., and Bierkens, M. F.: Climate change will affect the Asian water towers, *Science*, 328, 1382-1385, 2010.

IPCC, C. C.: The Physical Science Basis. Contribution of Working Group I to the Fourth Assessment Report of the Intergovernmental Panel on Climate Change, Cambridge University Press, Cambridge, United Kingdom and New York, NY, USA, 996, 2007, 2007.

Kang, S., Wake, C. P., Dahe, Q., Mayewski, P. A., and Tandong, Y.: Monsoon and dust signals recorded in Dasuopu glacier, Tibetan Plateau, *Journal of Glaciology*, 46, 222-226, 2000.

Kang, S., Xu, Y., You, Q., Flügel, W. A., Pepin, N., and Yao, T.: Review of climate and cryospheric change in the Tibetan Plateau, *Environmental Research Letters*, 5, 015101, 2010.

Kaspari, S., Painter, T., Gysel, M., and Schwikowski, M.: Seasonal and elevational variations of black carbon and dust in snow and ice in the Solu-Khumbu, Nepal and estimated radiative forcings, *Atmospheric Chemistry and Physics Discussions*, 13, 33491-33521, 2013.

Lhermitte, S., Greuell, W., van Meijgaard, E., van Oss, R., van den Broeke, M., and van de Berg, W.: Greenland ice sheet surface albedo: trends in surface properties (2000-2011), EGU General Assembly Conference Abstracts, 2012, 12349,

Ming, J., Cachier, H., Xiao, C., Qin, D., Kang, S., Hou, S., and Xu, J.: Black carbon record based on a shallow Himalayan ice core and its climatic implications, *Atmospheric Chemistry and Physics*, 8, 1352, 2008.

Ming, J., Xiao, C., Du, Z., and Flanner, M. G.: Black Carbon in snow/ice of west China and its radiative forcing, *Advances in Climate Change Research*, 92, 114-123, 2009a.

Ming, J., Xiao, C. D., Cachier, H., Qin, D. H., Qin, X., Li, Z. Q., and Pu, J. C.: Black Carbon (BC) in the snow of glaciers in west China and its potential effects on albedos, *Atmospheric Research*, 92, 114-123, 2009b.

Ming, J., Xiao, C., Sun, J., Kang, S., and Bonasoni, P.: Carbonaceous particles in the atmosphere and precipitation of the Nam Co region, central Tibet, *Journal of Environmental Sciences*, 22, 1748-1756, 2010.

Ming, J., Du, Z., Xiao, C., Xu, X., and Zhang, D.: Darkening of the mid-Himalaya glaciers since 2000 and the potential causes, *Environmental Research Letters*, 7, 014021, 2012.

Ming, J., Wang, P., Zhao, S., and Chen, P.: Disturbance of light-absorbing aerosols on the albedo in a winter snowpack of Central Tibet, *Journal of Environmental Sciences*, 337, 2013a.

Ming, J., Xiao, C., Du, Z., and Yang, X.: An Overview of Black Carbon Deposition in High Asia Glaciers and its Impacts on Radiation Balance, *Advances in Water Resources*, 80-87, 2013b.

Mote, P. W., Parson, E. A., Hamlet, A. F., Keeton, W. S., Lettenmaier, D., Mantua, N., Miles, E. L., Peterson, D. W., Peterson, D. L., and Slaughter, R.: Preparing for climatic change: the water, salmon, and forests of the Pacific Northwest, *Climatic Change*, 61, 45-88, 2003.

Oki, T., and Kanae, S.: Global hydrological cycles and world water resources, *science*, 313, 1068-1072, 2006.

Painter, T. H., Barrett, A. P., Landry, C. C., Neff, J. C., Cassidy, M. P., Lawrence, C. R., McBride, K. E., and Farmer, G. L.: Impact of disturbed desert soils on duration of mountain snow cover, *Geophysical Research Letters*, 34, 2007.

Painter, T. H., Skiles, S. M., Deems, J. S., Bryant, A. C., and Landry, C. C.: Dust radiative forcing in snow of the Upper Colorado River Basin: 1. A 6 year record of energy balance, radiation, and dust concentrations, *Water Resources Research*, 48, 2012.

Riggs G, Hall D: MODIS snow and ice products, and their assessment and applications, *Land*

Remote Sensing and Global Environmental Change. Springer New York, 681-707, 2011.

Sorman, A., Akyürek, Z., Sensoy, A., Sorman, A., and Tekeli, A.: Commentary on comparison of MODIS snow cover and albedo products with ground observations over the mountainous terrain of Turkey, *Hydrol. Earth Syst. Sci.*, 11, 1353-1360, 2007.

Stroeve, J. C., Box, J. E., and Haran, T.: Evaluation of the MODIS (MOD10A1) daily snow albedo product over the Greenland ice sheet, *Remote Sensing of Environment*, 105, 155-171, 2006.

Sugden, D. E., and John, B. S.: Glaciers and landscape: a geomorphological approach, Edward Arnold London, 1976.

Tekeli, A. E., Sensoy, A., Sorman, A., Akyürek, Z., and Sorman, Ü.: Accuracy assessment of MODIS daily snow albedo retrievals with in situ measurements in Karasu basin, Turkey, *Hydrological processes*, 20, 705-721, 2006.

Wang, J., B. Ye, Y. Cui, X. He, and G. Yang: Spatial and temporal variations of albedo on nine glaciers in western China from 2000 to 2011, *Hydrol Process.*, doi:10.1002/hyp.9883, 2013

Wang, Q., Jacob, D., Fisher, J., Mao, J., Leibensperger, E., Carouge, C., Sager, P., Kondo, Y., Jimenez, J., and Cubison, M.: Sources of carbonaceous aerosols and deposited black carbon in the Arctic in winter-spring: implications for radiative forcing, *Atmospheric Chemistry and Physics*, 11, 12453-12473, 2011.

Warren, S.G., Wiscombe, W.J. A model for the spectral albedo of snow. II: Snow containing atmospheric aerosols. *J. Atmos. Sci* 37, 2734-2745, 1980.

Warren, S. G.: Can black carbon in snow be detected by remote sensing?, *Journal of Geophysical Research: Atmospheres*, 118, 779-786, 2013.

Wiscombe, W.J., Warren, S.G. A model for the spectral albedo of snow. I: Pure snow. *Journal of the atmospheric sciences* 37, 2712-2733, 1980.

Xu, B., Cao, J., Hansen, J., Yao, T., Joswiak, D. R., Wang, N., Wu, G., Wang, M., Zhao, H., and Yang, W.: Black soot and the survival of Tibetan glaciers, *Proceedings of the National Academy of Sciences*, 106, 22114-22118, 2009a.

Xu, B., Wang, M., Joswiak, D. R., Cao, J. J., Yao, T. D., Wu, G. J., Yang, W., and Zhao, H. B.: Deposition of anthropogenic aerosols in a southeastern Tibetan glacier, *J. Geophys. Res.*, 114, D17209, 10.1029/2008JD011510, 2009b.

Xu, B., Cao, J., Joswiak, D. R., Liu, X., Zhao, H., and He, J.: Post-depositional enrichment of black soot in snow-pack and accelerated melting of Tibetan glaciers, *Environmental Research Letters*, 7, 014022, 2012.

Yao, T., Thompson, L., Yang, W., Yu, W., Gao, Y., Guo, X., Yang, X., Duan, K., Zhao, H., and Xu, B.: Different glacier status with atmospheric circulations in Tibetan Plateau and surroundings, *Nature Climate Change*, 2, 663-667, 2012.

Zhang, G., Kang, S., Fujita, K., Huintjes, E., Xu, J., Yamazaki, T., Haginoya, S., Wei, Y., Scherer, D., and Schneider, C.: Energy and mass balance of Zhadang glacier surface, central Tibetan Plateau, *Journal of Glaciology*, 59, 137-148, 2013.

Table 1. Sampling information: Two expeditions were conducted in Zhadang glacier and samples (albedo, snow/ice) were collected under three melting conditions of the glacier, in July and August of 2012. We measured the albedo five to six times at each site whilst collecting two to three snow/ice samples. In total, 120 albedo measurements and 48 snow/ice samples were obtained at the A - D sample site in Jul., 2012 for S-I and S-II conditinos (Fig. 2). A total of 160 albedo samples and 64 snow samples were obtained at all sampling sites in August 2012. The albedo and concentrations of BC and dust are listed here.

Sample date	Sample site	Altitude (m a.s.l.)	Number of samples (albedo/snow&ice)	Average of albedo	Average of BC conc. (ppb)	Average of dust conc. (ppm)	Snow grain size (mm)	Snowpack density (kg/m ³)	Snowpack Thickness (cm)	Solar zenith angle (°)	Cloud Amount (10=100%)	Scene type
July, 2012	A	5507	30/12	0.385	472.6	503.8	0.8 ~ 1.6	289 ~ 380	1	44.8~78.9	3~10	S-I
	B	5680	30/12	0.521	334.4	1891.9	0.6 ~ 1.6	289 ~ 350	1~2	52.3~75.8	1~10	
	C	5720	30/12	0.676	142.9	66.6	0.4 ~ 0.7	333 ~ 378	2~3	62.9~79.1	1~10	S-II
	D	5795	30/12	0.686	80.9	33.6	0.3 ~ 0.5	267~289	3	67.1~67.3	0~10	
August, 2012	A	5507	20/8	0.589	53.2	8.2	0.2 ~ 0.5	278 ~ 300	1~2	33.4~44	0~10	S-III
	B	5560	20/8	0.696	40.8	8.0	0.2 ~ 0.4	256 ~ 289	2~3	37.6~47.1	1~7	
	C	5626	20/8	0.710	55.5	7.0	0.2 ~ 0.4	267~311	2~3	40.8~50.2	0~7	
	D	5680	20/8	0.699	52.7	6.7	0.2 ~ 0.4	267~289	3	43.8~54.1	1~8	
	E	5695	20/8	0.708	55.2	6.4	0.2 ~ 0.4	267~289	3~4	45.8~57.9	0~6	
	F	5715	20/8	0.667	57.7	6.2	0.2 ~ 0.4	278~289	4	49.9~61.4	0~7	
	G	5750	20/8	0.698	59.4	5.2	0.2 ~ 0.3	222~244	5	51.9~64.6	0~7	
	H	5795	20/8	0.724	40.9	3.4	0.2 ~ 0.3	211~222	5	61.2~68.4	0~10	

Table 2. Sensitivity analysis with SNICAR model. BC% and dust% are the contributions of BC and dust to the total reduction of albedo, respectively. $R_{\text{in-short}}$ is the incident solar radiation measured by AWS.

Date	Site	OA*	SA** pure	SA +BC	SA +BC & dust	BC%	dust%	$R_{\text{in-short}}$	RF +BC	RF +dust	Scene type
15 July	A	0.385	0.406	0.395	0.388	52	33	780.1	8.6	5.5	S-I
16 July	A	0.387	0.413	0.405	0.396	31	34	412.6	3.3	3.7	
15 July	B	0.363	0.406	0.394	0.364	28	70	548.2	6.6	16.4	
16 July	B	0.558	0.577	0.576	0.560	4	85	535.3	0.4	8.6	
14 July	C	0.618	0.640	0.631	0.624	41	32	1308.5	11.8	9.2	S-II
15 July	C	0.723	0.758	0.742	0.727	46	43	543.7	8.7	8.2	
16 July	C	0.745	0.756	0.754	0.752	18	18	604.4	1.2	1.2	
14 July	D	0.745	0.771	0.760	0.753	42	27	552.7	6.1	3.9	
15 July	D	0.732	0.754	0.745	0.740	41	23	648.4	5.8	3.2	
16 July	D	0.755	0.775	0.770	0.764	25	30	789.8	3.9	4.7	
24 Aug	A	0.568	0.791	0.786	0.784	2	1	337.8	1.4	0.7	S-III
25 Aug	A	0.653	0.682	0.681	0.680	5	2	658.7	0.9	0.5	
26 Aug	A	0.716	0.746	0.739	0.737	23	7	702.5	4.9	1.4	
24 Aug	B	0.759	0.793	0.779	0.778	41	4	608.1	8.5	0.9	
25 Aug	B	0.696	0.731	0.728	0.727	8	4	722.7	1.9	0.9	
26 Aug	B	0.656	0.683	0.681	0.68	7	4	736.2	1.5	0.7	
26 Aug	C	0.697	0.734	0.732	0.732	5	1	776.8	1.6	0.3	
24 Aug	D	0.726	0.806	0.797	0.795	11	3	822.6	7.4	1.6	
25 Aug	D	0.768	0.781	0.780	0.778	17	10	814	1.8	1.1	
26 Aug	D	0.647	0.781	0.779	0.778	1	1	811	1.3	1.0	
24 Aug	E	0.699	0.810	0.803	0.802	6	1	962	6.7	1.0	
25 Aug	E	0.780	0.813	0.809	0.807	12	6	891.5	3.6	1.8	
26 Aug	E	0.774	0.811	0.805	0.804	16	3	831	5.0	1.0	
24 Aug	F	0.792	0.839	0.835	0.833	9	4	786.8	3.1	1.6	
25 Aug	F	0.790	0.819	0.816	0.815	10	3	1030	3.1	1.0	
26 Aug	F	0.566	0.816	0.809	0.808	3	1	895	6.0	1.2	
24 Aug	G	0.795	0.848	0.840	0.838	15	4	1303	10.4	2.6	
25 Aug	G	0.806	0.828	0.824	0.823	18	5	1168	4.7	1.2	
26 Aug	G	0.652	0.819	0.812	0.811	4	1	932	6.5	0.9	
24 Aug	H	0.811	0.853	0.846	0.846	16	1	1134	7.5	0.6	
25 Aug	H	0.809	0.834	0.831	0.830	12	4	1316	3.9	1.3	
26 Aug	H	0.711	0.827	0.825	0.824	2	1	1192	2.4	1.2	
Avg.	S-I,II,III	0.684	0.741	0.735	0.731	18	15	826.1	4.7	2.8	

* OA denotes observed abbedo. ** SA denotes simulated albedo.

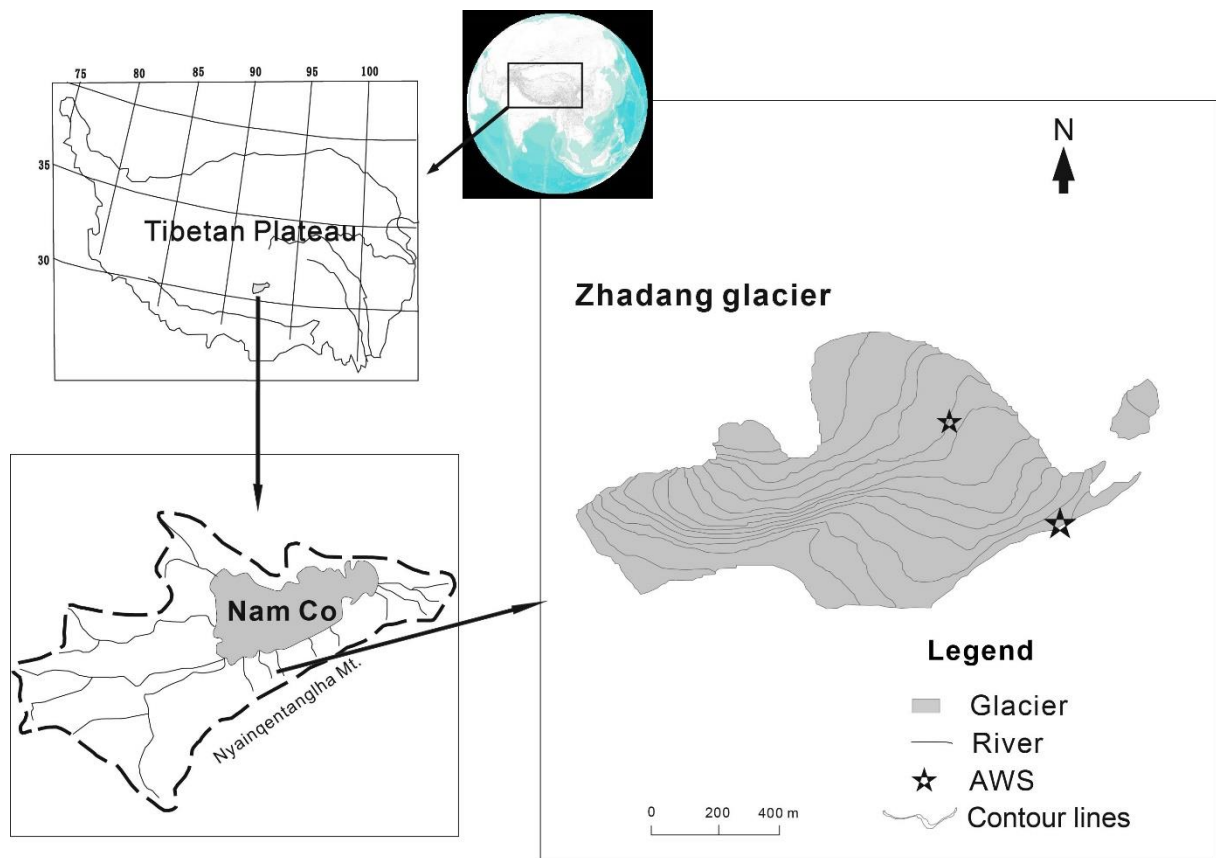


Figure 1. Location of Zhangdang glacier on Mt. Nyainqntanglha.

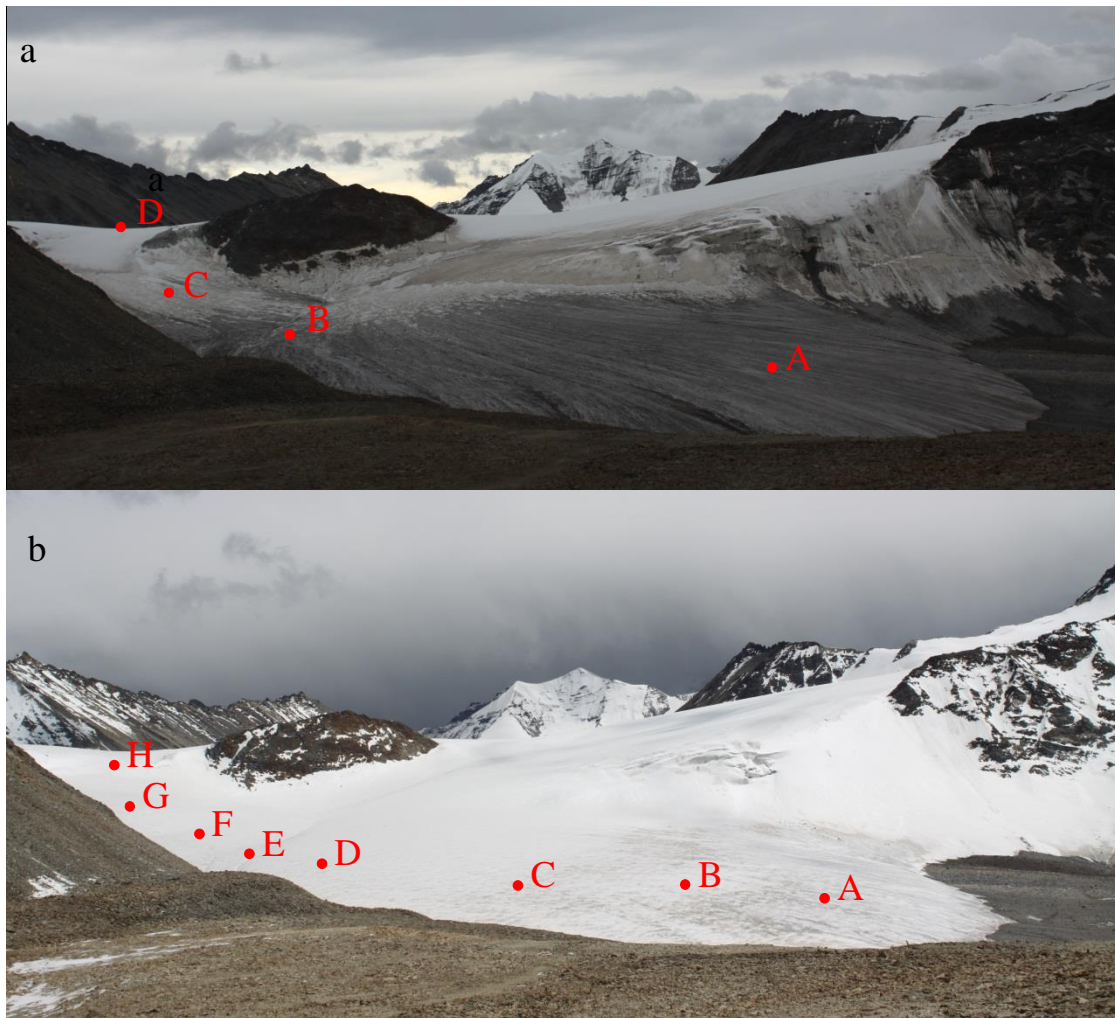


Figure 2. Surface features of Zhadang glacier on 16th Jul. (a) and 26th Aug. (b). The two surface conditions include three types of melting scenes: S-I: Sites A and B which are located in the superimposed ice belt (Fig.2a); S-II: Sites C and D which are in the upper area of the glacier (Fig.2a); S-III: All sites were covered by fresh snow (Fig.2b).

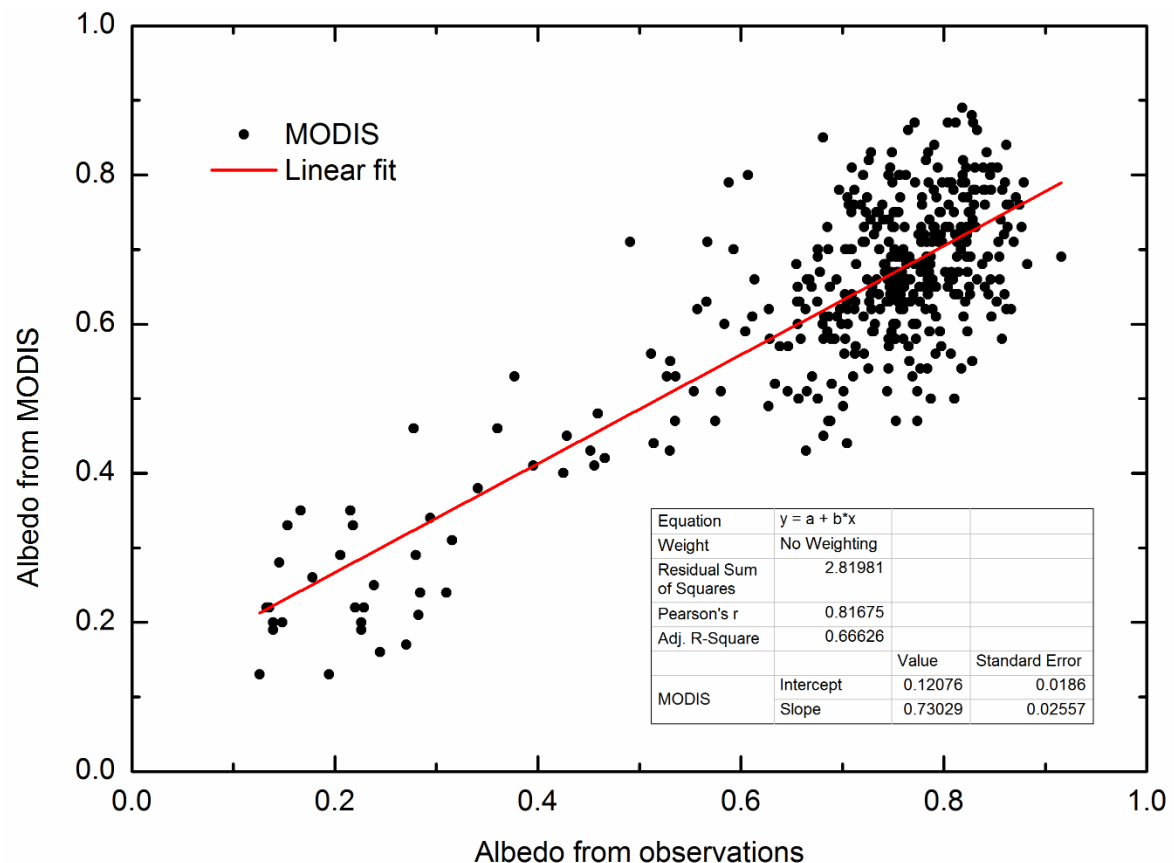


Figure 3. The albedo of the pixel including AWS in Zhadang glacier derived from MODIS and that observed by AWS in 2011.

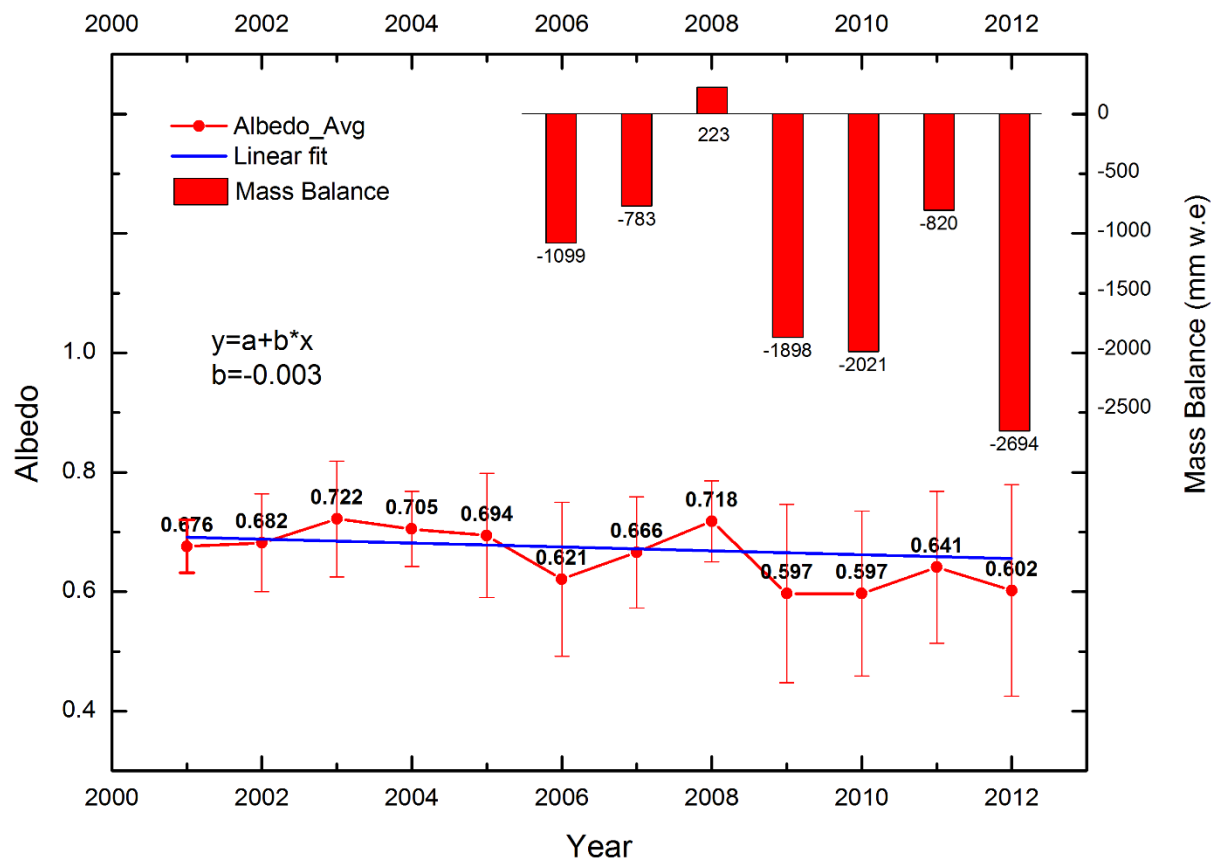


Figure 4. Temporal changes of albedo in Zhadang glacier during 2000 to 2012 and mass balance from 2006 to 2012. The albedo of Zhadang glacier showed a downward trend in the last decade overall. There is a significant positive correlation between albedo and the negative mass balance ($R^2 > 0.83$, passed the statistical significance test at 0.01 level).

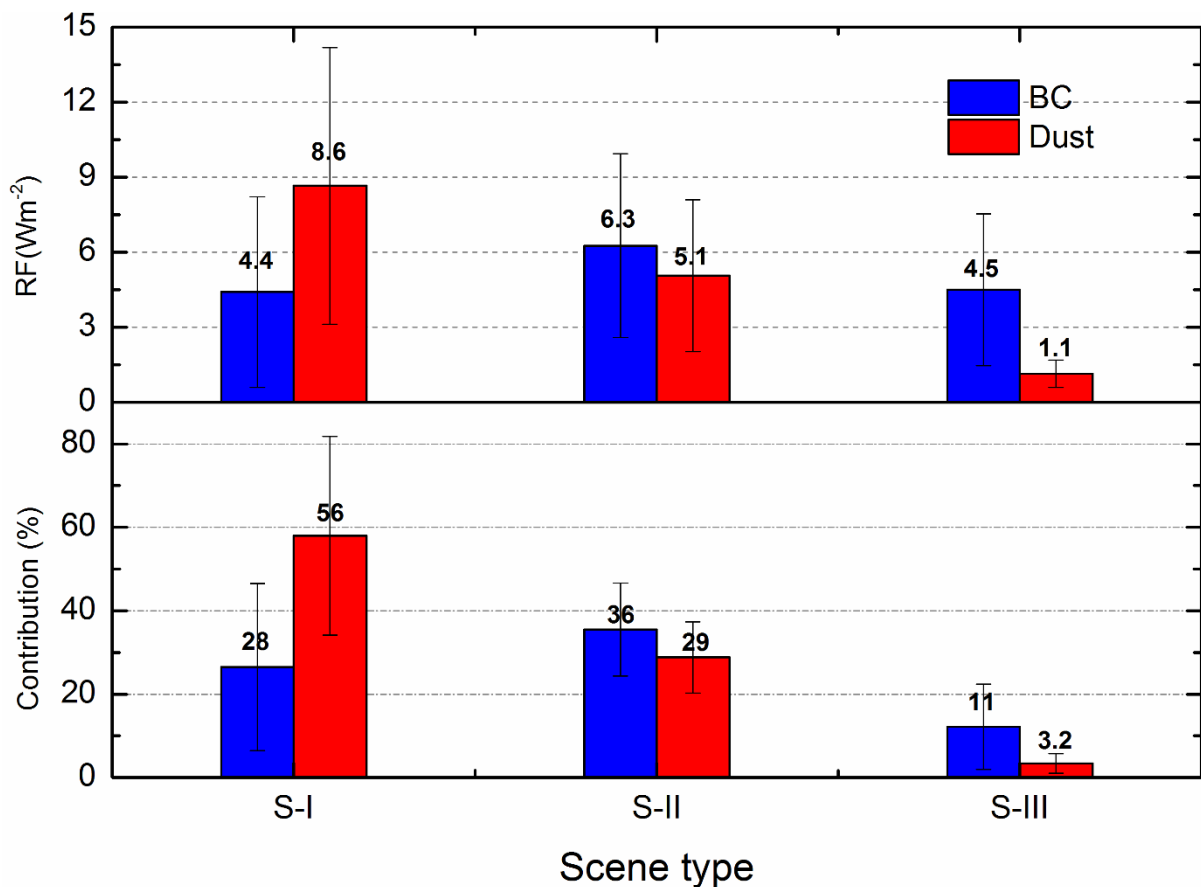


Figure 5. Mid-day RFs of BC and dust on the Zhadang glacier and the contribution (results from SNICAR model) show the reduction of albedo in the surface snow cover area under three different melting conditions: S-I, where the surface of the glacier is bare ice; S-II, where the glacier is covered by aged snow; S-III, where the glacier is covered by fresh snow.

Appendix

Parameters for sensitivity analysis with SNICAR

1. Incident radiation (a. Direct, b. Diffuse); 2. Solar zenith angle; 3. Surface spectral distribution (a. Mid-latitude winter, clear-sky, cloud amount < 5. b. Mid-latitude winter, cloudy, cloud amount ≥ 5); 4. Snow grain effective radius (μm); 5. Snowpack thickness (m); 6. Snowpack density (kg/m^3); 7. Albedo of underlying ground (a. Visible, 0.3–0.7 μm . b. Near-infrared, 0.7–5.0 μm); 8. MAC scaling factor (experimental) for BC; 9. Black carbon concentration (ppb, Sulfate-coated); 10. Dust concentration (ppm, 5.0–10.0 μm diameter); 11. Volcanic ash concentration (ppm); 12. Experimental particle 1 concentration (ppb)

Date	site	1	2	3	4	5	6	7a	7b	8	9	10	11	12
14, July	C	b	79.1	b	600	0.02	378	0.15	0.3	11	129.9	56.4	0	0
14, July	D	b	67.3	b	400	0.05	289	0.15	0.3	11	77.2	29.6	0	0
15, July	A	b	78.9	b	800	0.01	289	0.13	0.12	11	608.2	649.3	0	0
15, July	B	b	75.8	b	800	0.01	289	0.13	0.12	11	657.3	3628.8	0	0
15, July	C	a	71.6	a	400	0.02	367	0.15	0.3	11	278	135.1	0	0
15, July	D	a	67.2	a	400	0.03	278	0.15	0.3	11	114	39	0	0
16, July	A	a	44.8	a	700	0.01	380	0.13	0.12	11	337	358.3	0	0
16, July	B	a	52.3	a	700	0.02	350	0.15	0.3	11	11.5	155	0	0
16, July	C	a	62.9	b	400	0.03	333	0.15	0.3	11	20.8	8.3	0	0
16, July	D	a	67.1	a	400	0.04	267	0.15	0.3	11	51.5	32.2	0	0
24, Aug	A	b	44	b	250	0.03	300	0.13	0.12	11	60.2	9.6	0	0
24, Aug	B	a	47.1	b	200	0.03	289	0.13	0.12	11	153.6	8.2	0	0
24, Aug	C	a	50.2	b	200	0.02	311	0.13	0.12	11	111.4	9	0	0
24, Aug	D	a	54.1	a	200	0.03	289	0.13	0.12	11	115.4	8.1	0	0
24, Aug	E	a	57.9	a	200	0.03	267	0.15	0.3	11	87.6	7.7	0	0
24, Aug	F	a	61.4	a	200	0.04	289	0.15	0.3	11	41.3	9.1	0	0
24, Aug	G	a	64.6	b	200	0.05	244	0.15	0.3	11	84.7	7.1	0	0
24, Aug	H	a	68.4	b	200	0.05	222	0.15	0.3	11	67.9	2.6	0	0
25, Aug	A	a	33.4	a	250	0.02	278	0.13	0.12	11	29.2	5.9	0	0
25, Aug	B	a	37.6	a	200	0.02	278	0.13	0.12	11	43.2	9.1	0	0
25, Aug	C	a	40.8	b	200	0.03	311	0.13	0.12	11	32.2	6.1	0	0
25, Aug	D	a	43.9	b	200	0.03	267	0.13	0.12	11	22.5	6.8	0	0
25, Aug	E	a	47	b	200	0.04	289	0.15	0.3	11	31.4	6.3	0	0
25, Aug	F	a	52	b	200	0.04	278	0.15	0.3	11	28.3	4.1	0	0
25, Aug	G	a	54	b	200	0.05	244	0.15	0.3	11	33.4	3.2	0	0
25, Aug	H	a	61.2	b	200	0.05	211	0.15	0.3	11	33.6	5.6	0	0
26, Aug	A	a	37.5	b	250	0.03	289	0.13	0.12	11	70.2	9.2	0	0
26, Aug	B	a	39.6	a	250	0.02	256	0.13	0.12	11	38.3	6.8	0	0
26, Aug	C	a	41.7	b	200	0.02	267	0.13	0.12	11	23	5.9	0	0
26, Aug	D	a	43.8	a	200	0.03	267	0.13	0.12	11	20.3	5.2	0	0
26, Aug	E	a	45.8	b	200	0.04	289	0.15	0.3	11	46.6	5.2	0	0

26, Aug	F	a	49.9	b	200	0.04	278	0.15	0.3	11	57.7	5.5	0	0
26, Aug	G	a	51.9	b	200	0.05	222	0.15	0.3	11	60	5.4	0	0
26, Aug	H	b	62.6	b	200	0.05	211	0.15	0.3	11	21.1	2.1	0	0

SNICAR online, <http://snow.engin.umich.edu/>